Electronic Supplementary Material (ESI) for ChemComm.

Supporting Information for

Electrode Adsorption Activates *trans*-[Cr(cyclam)Cl_2]$^+$ for Electrocatalytic Nitrate Reduction

Sarah E. Braley, Daniel C. Ashley, Elena Jakubikova, and Jeremy M. Smith

Contents

Experimental Section

General Considerations. All anaerobic manipulations, including non-aqueous electrochemical measurements, were performed under a nitrogen atmosphere using standard Schlenk techniques or in an MBraun Labmaster glovebox. Deionized water was used for all aqueous experiments or measurements. All reagents were purchased from commercial venders and used as received. UV-visible spectra were recorded with an Agilent Cary 60 UV-visible spectrometer. Mass spectra were recorded using positive electrospray ionization on a Thermo Electron Corp MAT-95XP spectrometer. Nitrite, ammonia, and hydroxylamine were analyzed according to literature protocols.[1] Potentiometric titrations were performed at 25.0 ºC on a Mettler Toledo pH meter. The NaOH solutions for titration experiments were freshly prepared using deionized water to minimize carbonate formation.

Electrochemical Methods. Electrochemical measurements were recorded on a CHI 600D electrochemical analyzer (CH Instruments). Cyclic voltammetry experiments were carried out in an argon purged, air-tight, single compartment cell while controlled-potential experiments (CPE) electrolysis experiments were carried out in a two-compartment cell. Working electrode: glassy carbon electrode (3 mm diameter, CH Instruments) for cyclic voltammetry, carbon rod electrode (0.5 cm in diameter, 5 cm in length) for CPE. Auxiliary electrode: platinum wire (Alfa Aesar, 99.99%). Pseudo-reference electrode: Ag wire (Alfa Asear, 99.99%) for non-aqueous solution and Ag/AgCl (CH Instruments, 1M KCl, −0.006 V *vs*. SCE) for aqueous solution.

Experiments with a mercury pool working electrode were performed in a custom-made pear-shaped cell. Elemental mercury (≥ 99.99 % trace metals basis) was obtained from Sigma Aldrich and used without further purification. A platinum stick wire (Alfa Aesar, 99.9 %, 14 cm) was washed with ultrapure H_2O and acetone and then heated over a Bunsen burner to remove

impurities. This was then passed through a disposable glass capillary, leaving a half centimeter platinum wire foot at the bottom, and inserted into the cell. To the cell was added 0.25 mL mercury to cover the platinum foot. The bulk solution was then added over the mercury surface with care to prevent contact with the platinum stick wire. Finally, the platinum auxiliary and Ag/AgCl reference electrodes were added and the solution was purged with Argon. CPE was run for approximately one hour at −1.0 V *vs*. SCE at purify the mercury surface. The reproducibility of all cyclic voltammetry experiments was verified by several repeated scans.

Synthesis of Compounds

trans-[Cr(cyclam)Cl_2]Cl was synthesized according to literature procedures.[2] A 2:1 ratio of cyclam:$CrCl_3 \cdot 6H_2O$ was found to be optimal for ensuring high yields of this isomer. The product was recrystallized as purple needles from a 1:1:1 H_2O: 0.1 M HCl: acetone mixture.[3] The spectroscopic properties are identical to those reported in the literature.[3]

Characterization of *trans*-[Cr(cyclam)Cl_2]Cl: UV/Vis $\lambda_{max}(H_2O)$/nm 572 ($\varepsilon/M^{-1}cm^{-1}$ 17), 410sh (33), 364 (39).[3] ESI-MS (MeOH): calcd for *trans*-[Cr(cyclam)Cl_2]$^+$: ($C_{10}H_{24}Cl_2CrN_4$) m/z: 322.08 (M^+, 100%), 324.07 (64), 323.08 (22), 326.07 (10), 325.07 (7), found 322.1, 324.1, 323.1, 326.1.

trans-[Cr(cyclam)$(NO_3)_2$]NO_3 was synthesized from *trans*-[Cr(cyclam)Cl_2]Cl by adapting the literature procedure for the *cis* isomer.[3] The spectroscopic properties are identical to those reported in the literature.[4]

Characterization of *trans*-[Cr(cyclam)$(NO_3)_2$]NO_3: ESI-MS (MeOH): calcd for *trans*-[Cr($C_{10}H_{23}N_4$)(NO_3)]$^+$: ($C_{10}H_{23}CrN_5O_3$) m/z: 313.12 (M^+, 100%), 314.12 (22), found 313.0, 314.0. IR (KBr pellet) ν_{NO}/cm^{-1} 1512, 1384, 1282.

Characterization Spectra

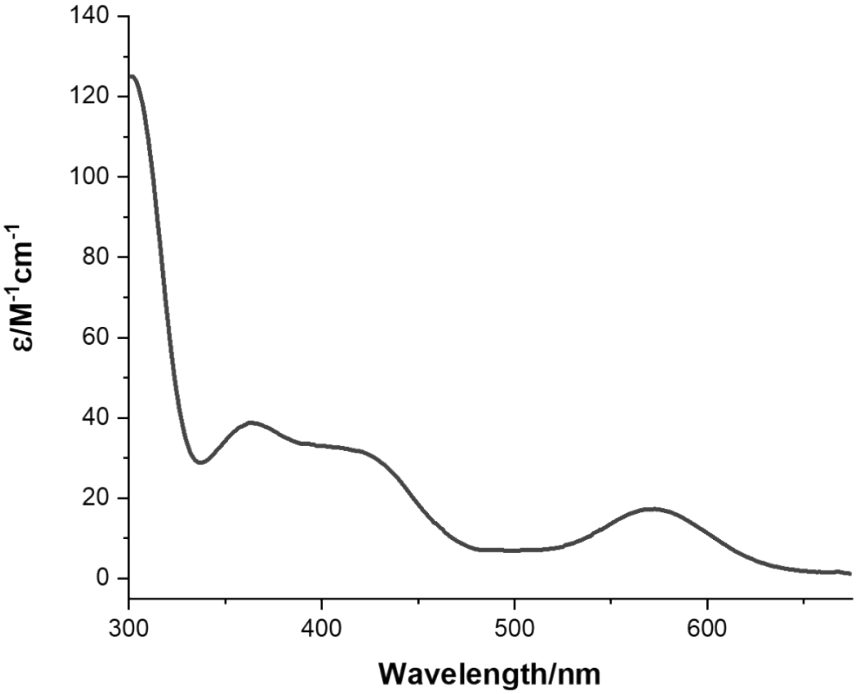

Figure S1: UV/Vis spectrum of *trans*-[Cr(cyclam)Cl_2]Cl in H_2O

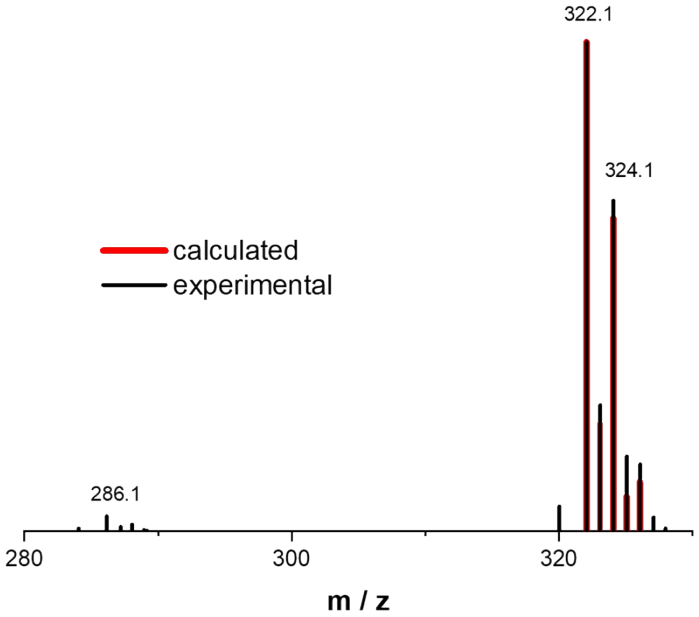

Figure S2: ESI MS of *trans*-[Cr(cyclam)Cl_2]Cl in H_2O. Experimental spectrum in black, calculated spectrum in red. Peak at m/z 288.0 can be attributed to $C_{10}H_{23}ClCrN_4^+$.

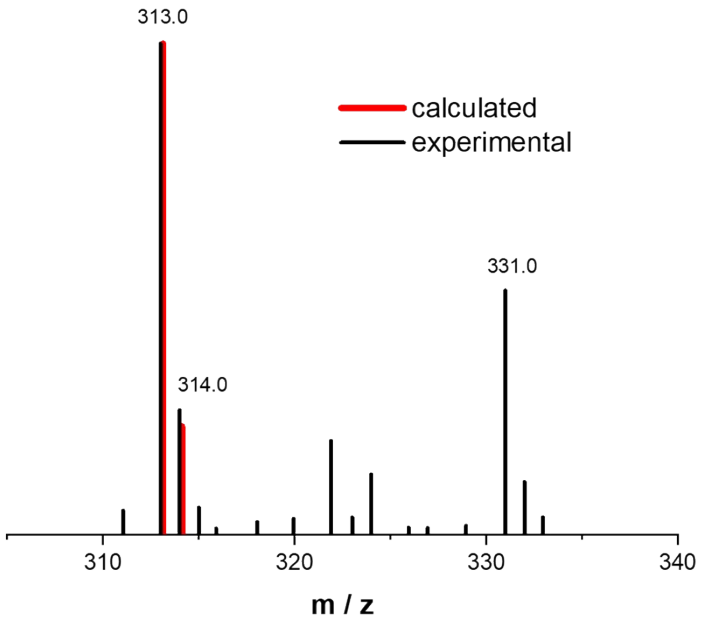

Figure S3: ESI MS of *trans*-[Cr(cyclam)$(NO_3)_2$](NO_3) in H_2O. Experimental spectrum in black, calculated spectrum in red. Peak at m/z 331.0 can be attributed to $[Cr(C_{10}H_{23}N_4)(NO_3)(H_2O]^+$.

Electrochemical Activity of *trans*-[Cr(cyclam)Cl_2]Cl

At a glassy carbon electrode in 0.1 M diethylpiperazine buffer (DEPP), *trans*-[Cr(cyclam)Cl_2]Cl undergoes an irreversible reduction with $E_{p,c}$ −1.47 V *vs*. SCE (**Figure S4**).

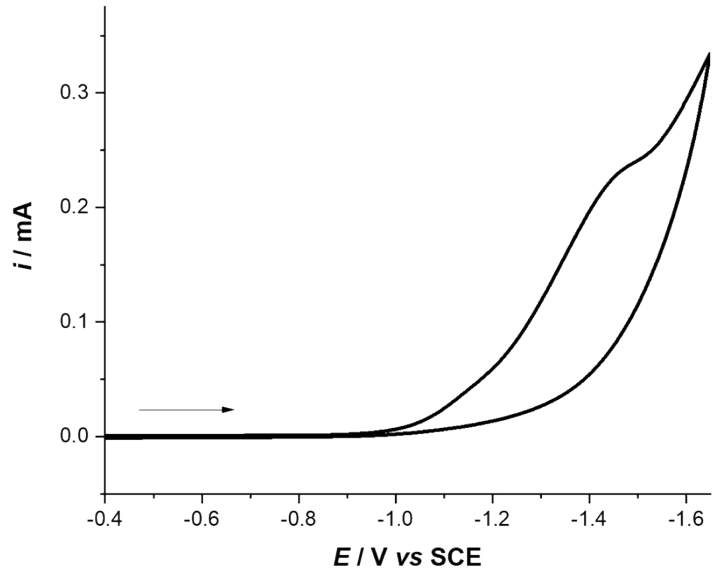

Figure S4: Cyclic voltammograms of 5 mM *trans*-[Cr(cyclam)Cl_2]Cl in 0.1 M DEPP pH 4.6 at glassy carbon, scan rate 50 mV/s.

Prewave Characterization

Varying the scan rate in cyclic voltammograms of *trans*-[Cr(cyclam)Cl_2]Cl at a mercury pool electrode shows that the peak current of the bulk wave varies with the square root of scan rate, while the peak current of the prewave varies directly with scan rate (**Figure S5**). This indicates that the prewave is due to a surface process.

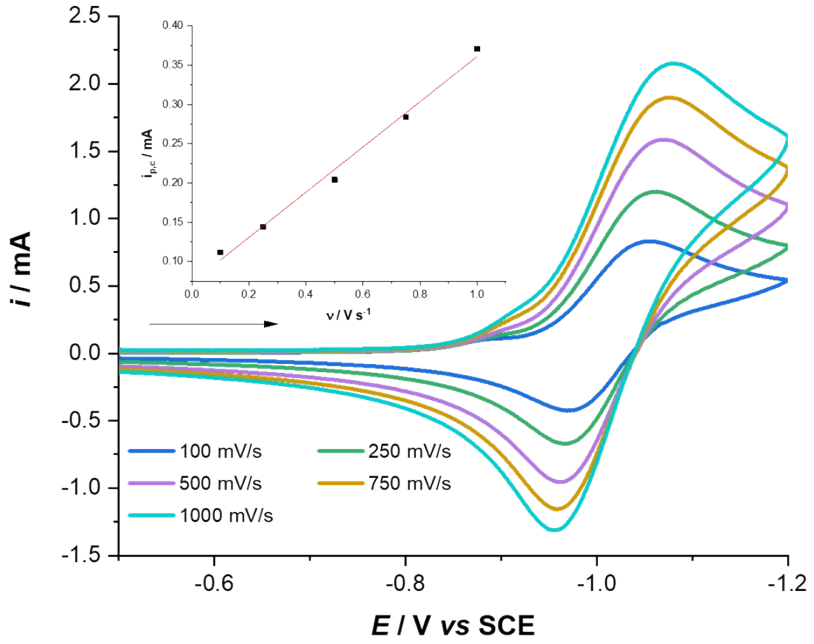

Figure S5: Cyclic voltammograms of 5 mM *trans*-[Cr(cyclam)Cl_2]Cl in 0.93 M DEPP buffer pH 4.6 at a mercury pool as scan rate is varied. Inset: plot of peak current *vs*. scan rate.

Electrocatalytic Activity of *trans*-[Cr(cyclam)Cl_2]Cl

Cyclic voltammograms of *trans*-[Cr(cyclam)Cl_2]Cl at a glassy carbon electrode in the presence of sodium nitrate shows catalytic current at a similar onset potential to that in the absence of substrate (**Figure S6**).

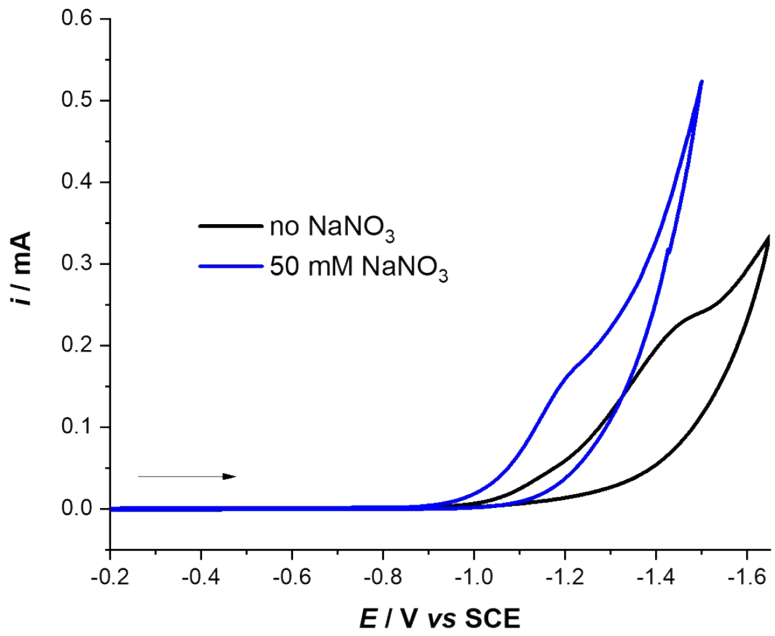

Figure S6: Cyclic voltammograms of 5 mM *trans*-[Cr(cyclam)Cl_2]Cl in 0.1 M DEPP buffer pH 4.6 at glassy carbon working electrode (black) and with 50 mM $NaNO_3$ (blue), scan rate 50 mV/s.

Cyclic voltammograms of *trans*-[Cr(cyclam)Cl_2]Cl at a mercury pool working electrode (**Figure S7**) shows a discrepancy in onset nitrate reduction potential of over 200 mV as compared to the glassy carbon electrode.

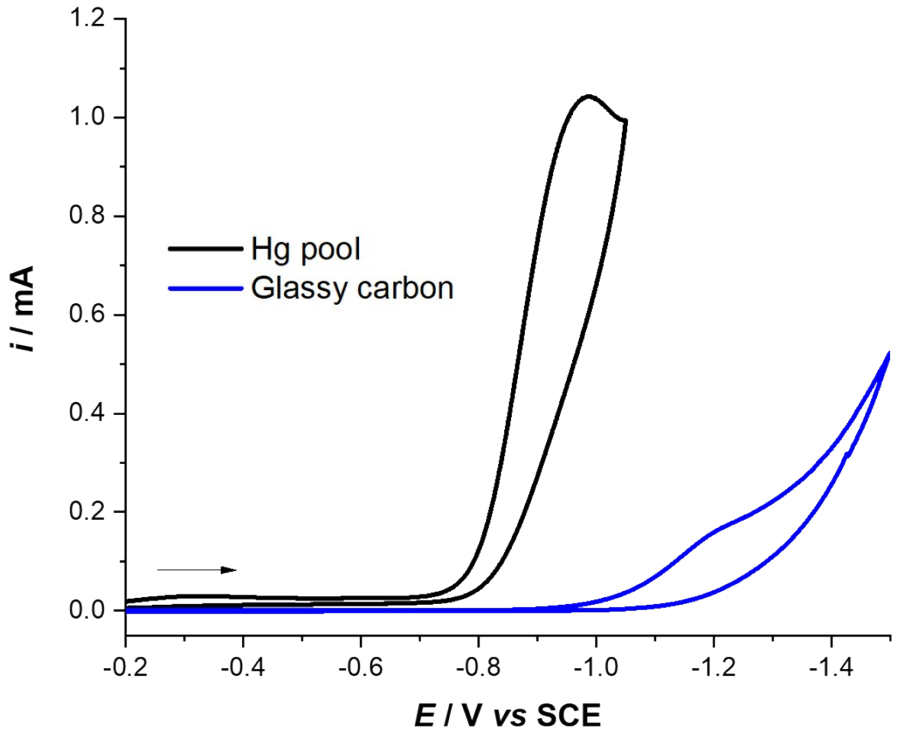

Figure S7: Cyclic voltammograms of 5 mM *trans*-[Cr(cyclam)Cl_2]Cl in 0.1 M DEPP buffer pH 4.6 at Hg pool working electrode (black) and glassy carbon working electrode (blue) in the presence of 50 mM $NaNO_3$, scan rate 50 mV/s.

Cyclic voltammograms of *trans*-[Cr(cyclam)Cl_2]Cl in the presence of $NaNO_2$ (**Figure S8**) show that the complex is also catalytic toward nitrite reduction. Tests for the presence of hydroxylamine and ammonia after controlled potential electrolysis show that neither is formed. Other gaseous products such as NO and N_2O are possible; this is still under investigation.

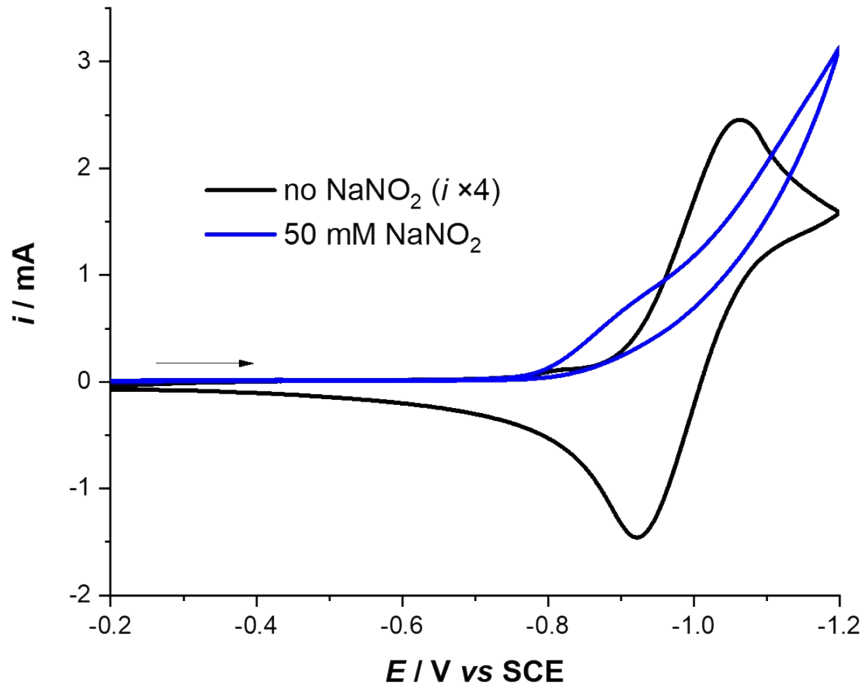

Figure S8: Cyclic voltammograms of 5 mM *trans*-[Cr(cyclam)Cl_2]Cl in 0.1 M DEPP buffer pH 4.6 at Hg pool working electrode (black) and with 50 mM $NaNO_2$ (blue), scan rate 50 mV/s.

Electrochemical Activity of *trans*-[Cr(cyclam)Cl_2]PF_6 in Organic Solvent

At a mercury pool electrode in acetonitrile, the onset potential is more negative than in water (**Figure S9**). No prewave is observed in acetonitrile.

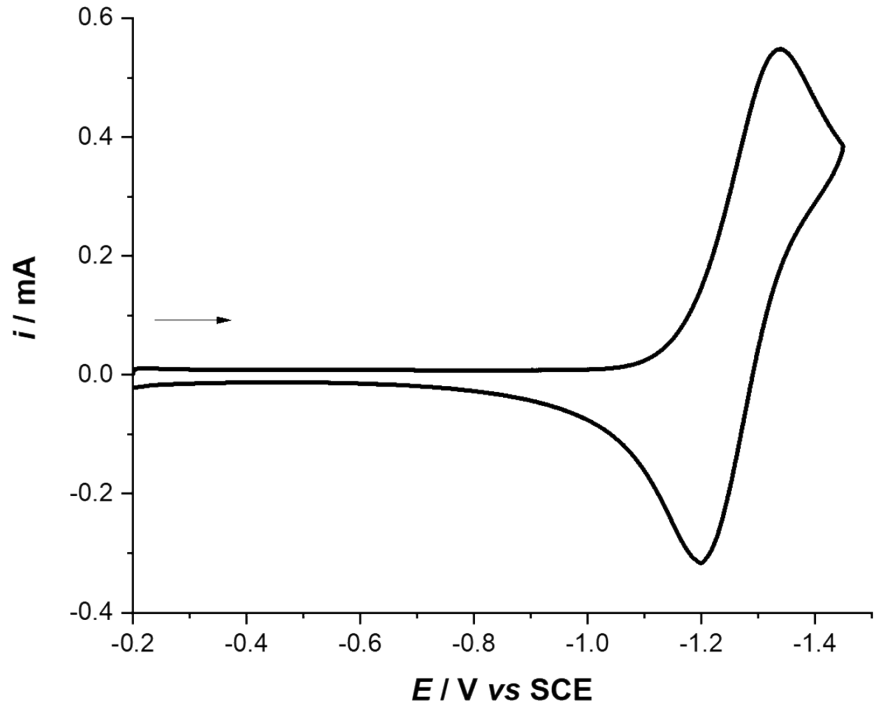

Figure S9: Cyclic voltammograms of 2 mM *trans*-[Cr(cyclam)Cl_2]PF_6 in 0.1 M $TBAPF_6$ at Hg pool working electrode, scan rate 50 mV/s.

Electrochemical Activity of *trans*-[Cr(cyclam)$(NO_3)_2$]NO_3

Figure S10 shows the change in onset reduction potential for *trans*-[Cr(cyclam)$(NO_3)_2$]NO_3 upon changing from a glassy carbon to a mercury pool electrode (current at the glassy carbon electrode has been multiplied by 2 to make it visually comparable to Hg pool).

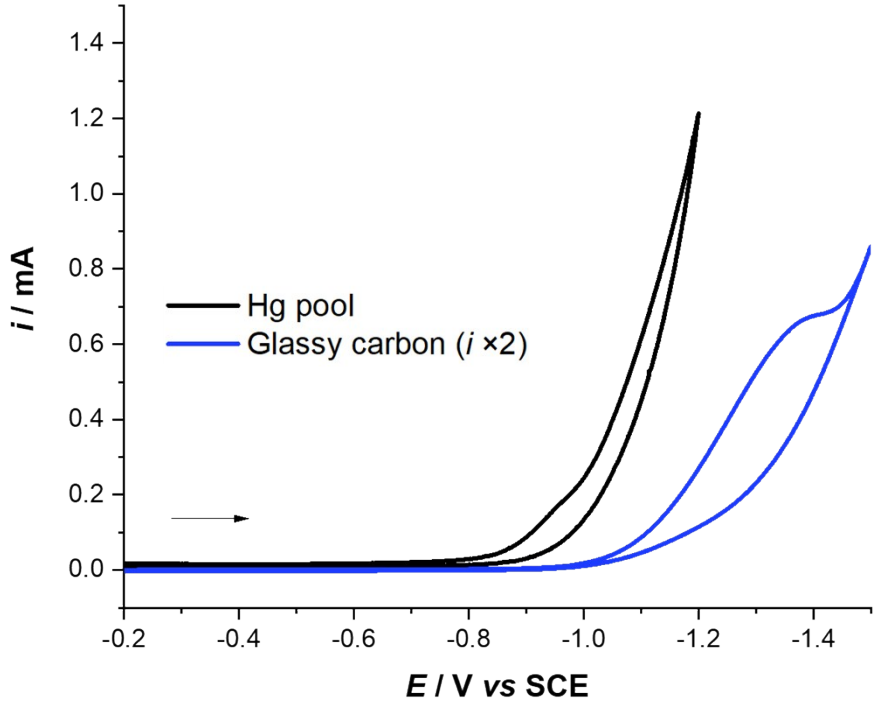

Figure S10: Cyclic voltammograms of 5 mM *trans*-[Cr(cyclam)$(NO_3)_2$]NO_3 in 0.1 M DEPP buffer pH 4.6 at Hg pool working electrode (black) and glassy carbon working electrode (blue), scan rate 50 mV/s.

Electrochemical Calculations

Faradaic efficiency: The amount of nitrite produced by CPE at −0.98 V or −1.13 V *vs*. Ag/AgCl was measured by the Griess method.[1c] Solution for CPE of *trans*-[Cr(cyclam)Cl_2]Cl at −0.98 V: 5 mM *trans*-[Cr(cyclam)Cl_2]Cl, 0.5 M Na_2SO_4, 75 mM $NaNO_3$ in H_2O (10 mL), pH = 6.16 (**Figure S11**). Nitrite quantification shows 80.5 µM nitrite produced over 1 hour CPE. According to equation 1, where n e^- is the number of electrons in the process (two, as shown in equation 2),

$$FE = \frac{(ne^-)F(molNO_2^-)}{Q} \#(1)$$

$$NO_3^- + 2H^+ + 2e^- \rightarrow NO_2^- + H_2O \#(2)$$

mol NO_2^- is the moles of nitrite produced in CPE, and Q is the charge consumption, the Faradaic efficiency can be calculated as:

$$FE = \frac{(2\,e^-)F(8.05 \times 10^{-7} mol)}{(0.15906\,C)} = 97.6\%$$

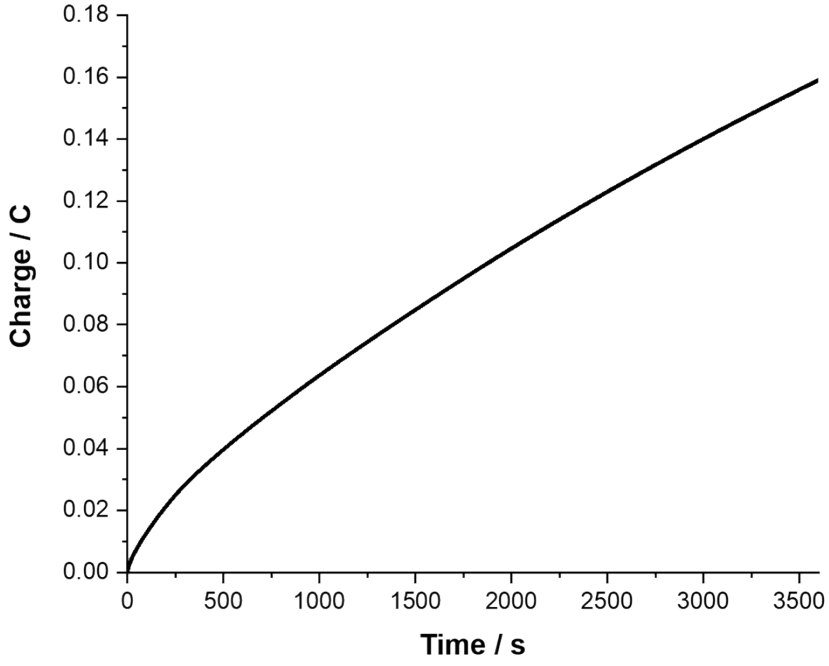

Figure S11: Bulk electrolysis of 5 mM *trans*-[Cr(cyclam)Cl_2]Cl in 0.5 M Na_2SO_4 at Hg pool working electrode with 75 mM $NaNO_3$, 1 hour at −0.98 V.

Phosphine Oxidation

Bulk electrolysis was performed in the presence of triphenylphosphine-3,3′,3″-trisulfonic acid trisodium salt (**Figure S12**). Bulk electrolysis solution contained 0.5 M Na_2SO_4, 25 mM $NaNO_3$, 5 mM *trans*-[Cr(cyclam)Cl_2]Cl, and 25 mM phosphine. This was electrolyzed at −0.98 V for 1 h, and $^{31}P\{^1H\}$ NMR was taken before and after (**Figure S13**). At time zero, phosphine oxide (34.25 ppm) accounts for 9 % of total sample. After 1 hour, conversion to 23 % phosphine oxide was observed. Bulk electrolysis controls in the absence of catalyst or nitrate show no conversion of phosphine to phosphine oxide.

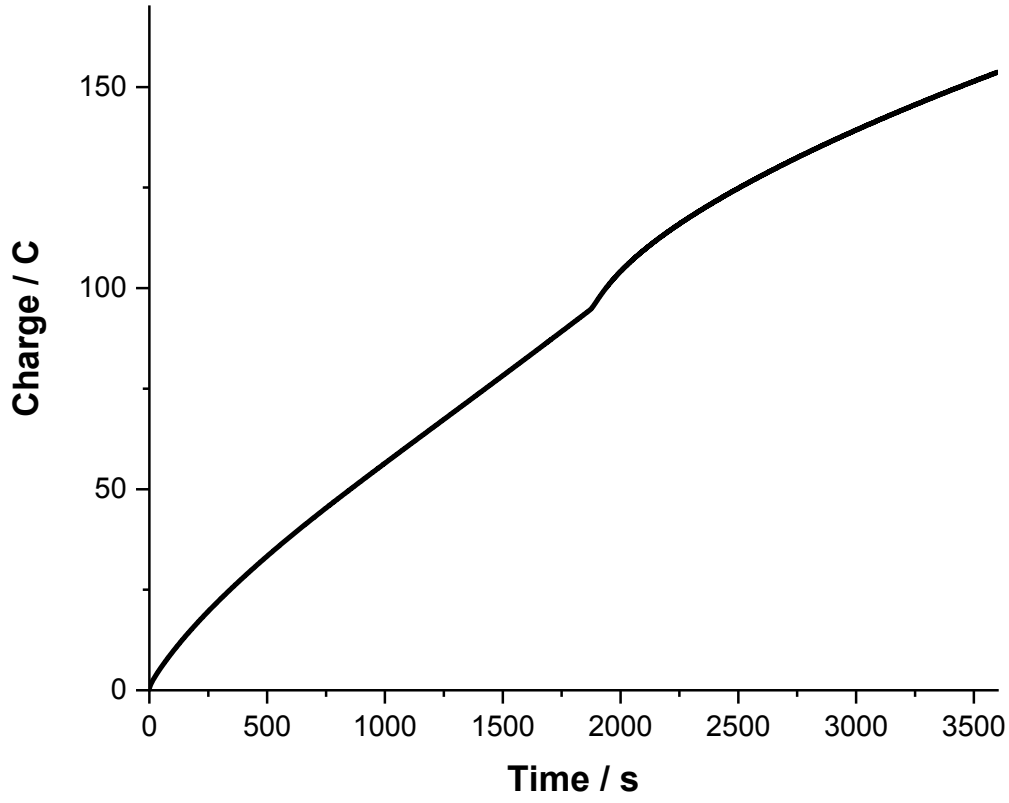

Figure S12: Bulk electrolysis of 5 mM *trans*-[Cr(cyclam)Cl_2]Cl in 0.5 M Na_2SO_4 at Hg pool working electrode with 25 mM $NaNO_3$ and 25 mM triphenylphosphine-3,3′,3″-trisulfonic acid trisodium salt, 1 hour at −0.98 V.

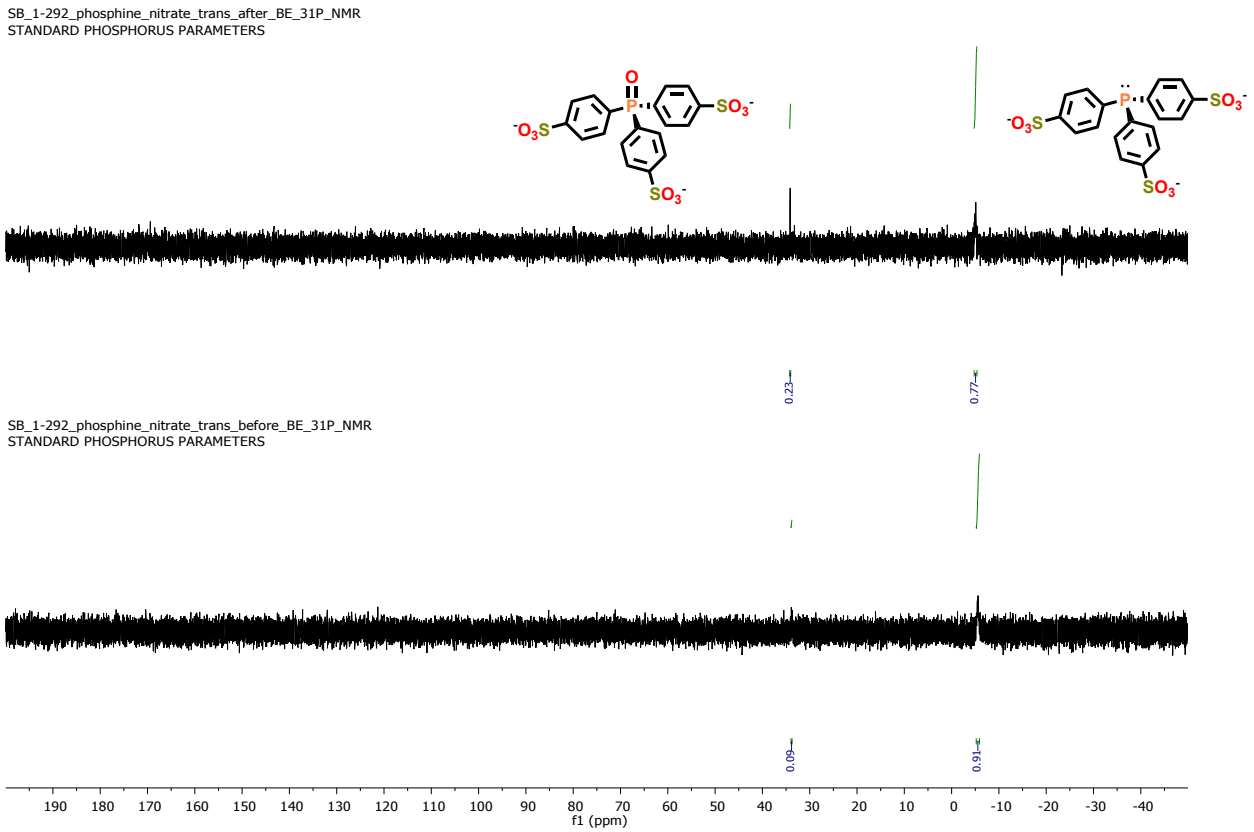

Figure S13: $^{31}P\{^{1}H\}$ NMR after (bottom) zero hours CPE and (top) 1 hour CPE at −0.98 $V_{Ag/AgCl}$.

The Faradaic efficiency for nitrite production is greatly decreased in the presence of phosphine (13 %). Only 15 μM nitrite is produced, which is less than the 3.5 mM phosphine oxide formed (from percent conversion in **Figure S13**). Finally, after longer CPE (12 h), a small amount of hydroxylamine formation is observed. These issues could indicate a different mechanism in the presence of phosphine.

Computational Methods

General Methodology

All DFT calculations were performed with the Gaussian 09 software package Revision D.01.[5] All calculations were performed using the B3LYP[6] functional including Grimme's D2 dispersion correction[7] (B3LYP+D2), and the implicit SMD[8] model to account for solvent effects (water). One exception was that the default PCM implicit solvation model was used for the chloride ion, as in previous work we found better results for bromide when using the PCM model.[9] All geometries were optimized, and vibrational frequencies were calculated for all optimized structures using the harmonic oscillator approximation to verify that the structures were true minima with no imaginary frequencies. These frequency calculations were also used to calculate zero-point energy (ZPE) and entropic corrections to the free energy (assuming a temperature and pressure of 298.15 K and 1.0 atm respectively) using standard statistical mechanical conventions. Wavefunction stability tests were performed on all complexes to verify that the electronic state converged to was stable.

A smaller, more affordable basis set (BS-I) was used for geometry optimizations and vibrational frequencies. Single point energy calculations were performed on these optimized energies using a larger basis set (BS-II) to determine the electronic energies. Both BS-I and BS-II employed the SDD basis set and pseudopotential for Cr.[10] All other atoms used 6-31G* for BS-I[11] and 6-311+G** for BS-II.[12] An ultrafine grid was used for all calculations. Finally, the solvated free energy (G_{sol}) was adjusted[13] to be at the standard state concentration of 1 M or 55.5 M for water, which amounted to a correction of 1.9 or 4.3 kcal/mol, respectively.

Cyclam is a highly flexible ligand, and as such for all cyclam-containing molecules numerous geometries had to be investigated. These included the multiple configurational isomers possible depending on the configuration about each coordinating amine (this amounts to five

diastereomers total) and also that the cyclam amines can either all be in the same plane, the trans configuration (in reference to the orientation of the two remaining ligands) or the cyclam ligand can bend to form the cis configuration. Altogether, this entailed considering ten possible geometries for each cyclam complex. All Cr(III) cyclam complexes were considered in the quartet state and all Cr(II) complexes were considered to be in the quintet state (HS for each). For the Cr(IV) oxo species the triplet and quintet spin states were considered, and for every geometry the triplet was always considerably lower in energy (20-30 kcal/mol). The only structure reported for each complex is the lowest energy structure calculated; the various higher energy isomers evaluated were not reported.

Calculated reduction potentials (E^0) were determined relative to the normal hydrogen electrode (NHE) through equation 3:

$$E^0(eV) = -\frac{\Delta G_{sol}}{nF} - 4.28\#(3)$$

Here, ΔG_{sol} is the change in solvated free energy upon reduction, n is the number of electrons transferred, and F is Faraday's constant. The calculated potentials are referenced to NHE by subtracting the absolute reduction potential of NHE, 4.28 V.[14] The calculated values vs. NHE are then reported relative to SCE (0.2412 vs. NHE).[15] Note that there are various different estimates of the absolute value of NHE, not all of which agree,[14, 16] and hence our calculated values may be subject to a minor systematic error if 4.28 V is not the best estimate. This will have no significant effect on our major qualitative conclusions, however. More importantly, we were able to benchmark the methodology described above against experimentally known Cr(III) reduction potentials as shown below. This gave us an estimate for how, and how much our calculated reduction potentials might be in error.

Methodology Benchmarking

To evaluate our computational methodology reduction potentials were calculated for eight homoleptic Cr(III) complexes using the ligands shown in Scheme S1. Five of these ligands were amines (primary and secondary) while the remaining three were polypyridines. All Cr(III) species were treated as quartets (HS) and while both the triplet and quintet spin states were evaluated for Cr(II). It was found that in all cases the amine complexes preferred the HS state for Cr(II) while the polypyridine complexes preferred the LS state. All of these complexes have had their electrochemistry experimentally characterized.[17] All of the polypyridine complexes and the $Cr(tacn)_2$ have had E^0 experimentally determined. The remaining amine complexes have only had their reductive half waves (E_{red}) determined through polarography due to the lability of the resulting Cr(II) complexes. As such we do not have an actual reversible E^0 to compare to our calculations. It can be assumed that the E_{red} determined for these complexes will be more negative than the actual experimental reduction potential (if it were determined). We cannot say how much more negative these E_{red} will be compared to E^0, however. Table S1 lists the calculated E^0 values and the experimentally determined values (E^0 or E_{red}).

Two features are immediately apparent from the results shown in Table S1. The first is that our calculated results agree reasonably well with experiment, with errors on the order of ~0.2 eV, which is a typical error for DFT estimated reduction potentials.[9, 18] The second is that the error is consistent: for each Cr(III) complex examined, the calculated reduction potential is always more negative than the experimental value. For the complexes where only E_{red} is known this conclusion still holds true, as the calculated values are more negative than E_{red} and E_{red} is already more negative than the expected experimental value of E^0. This consistent error is important for the interpretation of the results in the main text as when it comes to matching a calculated value to an

experimentally observed one, it is reasonable to assume that the calculated value should be slightly more negative than the measured experimental value.

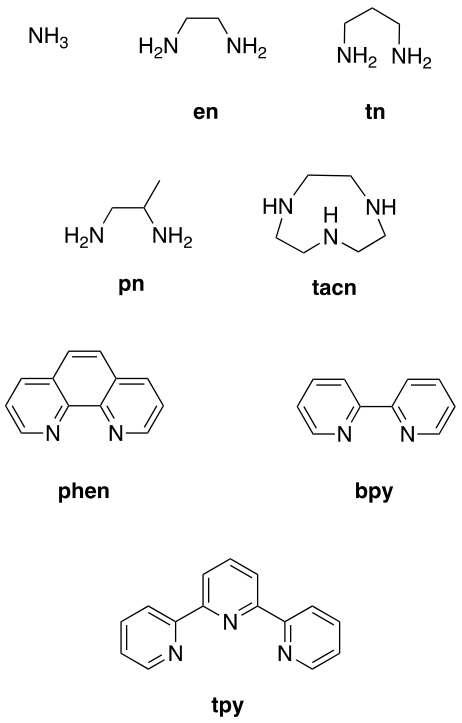

Scheme S1. Ligands employed in homoleptic Cr(III) complexes used for benchmarking the computational methodology.

Table S1. Calculated reduction potentials compared to experimentally measured E^0 or E_{red}. [a]Experimental value corresponds to E_{red}.

Ligands	E^0 or E_{red} (eV) Experimental[17]	E^0 (eV) Calculated	Signed error (eV)
$(NH_3)_6$[a]	-1.02	-1.15	-0.13
$(en)_3$[a]	-1.27	-1.37	-0.10
$(tn)_3$[a]	-1.1	-1.37	-0.27
$(pn)_3$[a]	-1.29	-1.45	-0.16
$(tacn)_2$	-1.38	-1.42	-0.04
$(phen)_3$	-0.52	-0.72	-0.20
$(bpy)_3$	-0.54	-0.77	-0.23
$(tpy)_2$	-0.41	-0.65	-0.24
Average	--	--	-0.17

Calculated Energies

Table S2. Electronic energies (E), zero-point energies (ZPE), entropic corrections to free energies (−TS), enthalpies (H, which includes other thermal corrections in addition to ZPE), and solvated Gibbs free energies (G_{sol}) calculated with DFT. Solvated free energies not adjusted for concentration are listed as G′. All optimizations were done with the SMD correction for water, hence E contains the solvation effects. The temperature (T) was set to 298.15 K, and the pressure to 1 atm. All values are reported in kcal/mol. The concentration of all species is considered to be 1 M with the exception of water, which is treated as 55.5 M.

Complex	E	ZPE	-TS	H	Gsol	G′
$[Cr(cyclam)Cl_2]^+$	-1018048.2	230.7	-39.2	-1017805.9	-1017843.3	-1017845.2
$Cr(cyclam)Cl_2$	-1018117.6	227.7	-43.9	-1017877.1	-1017919.2	-1017921.1
$[Cr(cyclam)Cl]^{2+}$	-729114.5	229.8	-37.2	-728874.1	-728909.3	-728911.2
$[Cr(cyclam)Cl]^+$	-729203.7	227.6	-39.6	-728964.8	-729002.6	-729004.5
$[Cr(cyclam)]^{3+}$	-440287.8	227.1	-36.5	-440050.7	-440085.3	-440087.2
$[Cr(cyclam)]^{2+}$	-440179.1	230.0	-34.7	-439939.7	-439972.5	-439974.4
$[Cr(cyclam)(NO_3)]^+$	-616348.6	236.8	-44.1	-616098.9	-616141.2	-616143.1
$[Cr(cyclam)O]^{2+}$	-487492.6	231.2	-36.5	-487251.1	-487285.8	-487287.7
H_2O	-47986.8	13.1	-13.9	-47971.4	-47980.9	-47985.2
Cl^-	-288914.6	0.0	-10.9	-288913.2	-288922.2	-288924.1
NO_3^-	-176051.6	8.7	-18.6	-176040.2	-176056.9	-176058.8
NO_2^-	-128847.4	4.9	-17.3	-128840.0	-128855.4	-128857.3
$[Cr(NH_3)_6]^{3+}$	-267535.5	151.2	-34.4	-267374.7	-267407.3	-267409.2
$[Cr(NH_3)_6]^{2+}$	-267601.2	143.7	-41.6	-267445.2	-267484.9	-267486.8
$[Cr(en)_3]^{3+}$	-413299.9	222.3	-35.8	-413067.7	-413101.6	-413103.5
$[Cr(en)_3]^{2+}$	-413365.1	217.2	-39.7	-413136.4	-413174.2	-413176.1
$[Cr(tn)_3]^{3+}$	-487343.0	278.9	-39.1	-487052.4	-487089.6	-487091.4

$[Cr(tn)_3]^{2+}$	-487405.8	272.2	-44.0	-487120.0	-487162.1	-487164.0
$[Cr(pn)_3]^{3+}$	-487347.2	273.8	-42.5	-487060.5	-487101.1	-487103.0
$[Cr(pn)_3]^{2+}$	-487411.3	269.4	-46.1	-487127.7	-487171.8	-487173.7
$[Cr(tacn)_2]^{3+}$	-559060.5	291.7	-37.7	-558757.8	-558793.6	-558795.5
$[Cr(tacn)_2]^{2+}$	-559126.0	287.6	-40.7	-558826.3	-558865.1	-558867.0
$[Cr(phen)_3]^{3+}$	-1130867.6	329.5	-58.1	-1130518.4	-1130574.6	-1130576.5
$[Cr(phen)_3]^{2+}$	-1130951.9	327.0	-59.4	-1130604.9	-1130662.4	-1130664.3
$[Cr(bpy)_3]^{3+}$	-987324.3	305.8	-56.3	-987000.0	-987054.5	-987056.4
$[Cr(bpy)_3]^{2+}$	-987408.6	303.5	-56.4	-987086.4	-987141.0	-987142.9
$[Cr(tpy)_2]^{3+}$	-986565.7	291.3	-54.3	-986256.6	-986309.0	-986310.9
$[Cr(tpy)_2]^{2+}$	-986652.1	289.2	-55.2	-986344.9	-986398.3	-986400.1

References

1. (a) Frear, D. S.; Burrell, R. C., *Anal. Chem.* **1955,** *27* (10), 1664-1665; (b) Weatherburn, M. W., *Anal. Chem.* **1967,** *39* (8), 971-974; (c) Mathews, J. E.; George, S.; Mathews, P.; Mathai, E.; Brahmadathan, K. N.; Seshadri, L., *Aust. New Zealand J. Obstet. Gynaecol.* **1998,** *38* (4), 407-410.
2. Bakac, A.; Espenson, J. H., *Inorg. Chem.* **1992,** *31* (6), 1108-1110.
3. Ferguson, J.; Tobe, M. L., *Inorg. Chim. Acta* **1970,** *4*, 109-112.
4. Kane-Maguire, N. A.; Wallace, K. C.; Miller, D. B., *Inorg. Chem.* **1985,** *24* (4), 597-605.
5. Frisch, M. J.; Trucks, G. W.; Schlegel, H. B.; Scuseria, G. E.; Robb, M. A.; Cheeseman, J. R.; Scalmani, G.; Barone, V.; Mennucci, B.; Petersson, G. A.; Nakatsuji, H.; Caricato, M.; Li, X.; Hratchian, H. P.; Izmaylov, A. F.; Bloino, J.; Zheng, G.; Sonnenberg, J. L.; Hada, M.; Ehara, M.; Toyota, K.; Fukuda, R.; Hasegawa, J.; Ishida, M.; Nakajima, T.; Honda, Y.; Kitao, O.; Nakai, H.; Vreven, T.; Montgomery, J. A., Jr.; Peralta, J. E.; Ogliaro, F.; Bearpark, M.; Heyd, J. J.; Brothers, E.; Kudin, K. N.; Staroverov, V. N.; Kobayashi, R.; Normand, J.; Raghavachari, K.; Rendell, A.; Burant, J. C.; lyengar, S. S.; Tomasi, J.; Cossi, M.; Rega, N.; Millam, N. J.; Klene, M.; Knox, J. E.; Cross, J. B.; Bakken, V.; Adamo, C.; Jaramillo, J.; Gomperts, R.; Stratmann, R. E.; Yazyev, O.; Austin, A. J.; Cammi, R.; Pomelli, C.; Ochterski, J. W.; Martin, R. L.; Morokuma, K.; Zakrzewski, V. G.; Voth, G. A.; Salvador, P.; Dannenberg, J. J.; Dapprich, S.; Daniels, A. D.; Farkas, Ö.; Foresman, J. B.; Ortiz, J. V.; Cioslowski, J.; Fox, D. J. *Gaussian 09, Rev D.01*, Gaussian 09, revision D.01; Gaussian, Inc.: Willingford CT, 2009.
6. (a) Becke, A. D., *Phys. Rev. A* **1988,** *38* (6), 3098-3100; (b) Lee, C.; Yang, W.; Parr, R. G., *Phys. Rev. B* **1988,** *37* (2), 785-789; (c) Becke, A. D., *J. Chem. Phys.* **1993,** *98*, 5648-5652; (d) Becke, A. D., *J. Chem. Phys.* **1993,** *98* (2), 1372.
7. Grimme, S., *J. Comput. Chem.* **2006,** *27* (15), 1787-1799.
8. Marenich, A. V.; Cramer, C. J.; Truhlar, D. G., *J. Phys. Chem. B* **2009,** *113* (18), 6378-6396.
9. Xu, S.; Ashley, D. C.; Kwon, H.-Y.; Ware, G. R.; Chen, C.-H.; Losovyj, Y.; Gao, X.; Jakubikova, E.; Smith, Jeremy M., *Chem. Sci.* **2018,** *9* (22), 4950-4958.
10. Dolg, M.; Wedig, U.; Stoll, H.; Preuss, H., *J. Chem. Phys.* **1987,** *86* (2), 866-872.
11. (a) Hariharan, P. C.; Pople, J. A., *Thero. Chim. Acta* **1973,** *28* (3), 213-222; (b) Francl, M. M.; Pietro, W. J.; Hehre, W. J.; Binkley, J. S.; Gordon, M. S.; DeFrees, D. J.; Pople, J. A., *J. Chem. Phys.* **1982,** *77* (7), 3654-3665.
12. (a) Krishnan, R.; Binkley, J. S.; Seeger, R.; Pople, J. A., *J. Chem. Phys.* **1980,** *72* (1), 650-654; (b) McLean, A. D.; Chandler, G. S., *J. Chem. Phys.* **1980,** *72* (10), 5639-5648.
13. Cramer, C. J., *Essentials of Computational Chemistry: Theories and Models.* 2nd ed.; John WIley & Sons: 2004.
14. Kelly, C. P.; Cramer, C. J.; Truhlar, D. G., *J. Phys. Chem. B* **2006,** *110* (32), 16066-16081.
15. Bard, A. J.; Faulkner, L. R., *Electrochemical Methods: Fundamentals and Applications.* John Wiley & Sons: NY, 2000.
16. (a) Kelly, C. P.; Cramer, C. J.; Truhlar, D. G., *J. Phys. Chem. B* **2007,** *111* (2), 408-422; (b) Fawcett, W. R., *Langmuir* **2008,** *24* (17), 9868-9875; (c) Tissandier, M. D.; Cowen,

K. A.; Feng, W. Y.; Gundlach, E.; Cohen, M. H.; Earhart, A. D.; Coe, J. V.; Tuttle, T. R., *J. Phys. Chem. A* **1998,** *102* (40), 7787-7794; (d) Tissandier, M. D.; Cowen, K. A.; Feng, W. Y.; Gundlach, E.; Cohen, M. H.; Earhart, A. D.; Tuttle, T. R.; Coe, J. V., *J. Phys. Chem. A* **1998,** *102* (46), 9308-9308; (e) Zhan, C.-G.; Dixon, D. A., *J. Phys. Chem. A* **2001,** *105* (51), 11534-11540; (f) Reiss, H.; Heller, A., *J. Phys. Chem.* **1985,** *89* (20), 4207-4213.

17. (a) Serpone, N.; Jamieson, M. A.; Henry, M. S.; Hoffman, M. Z.; Bolletta, F.; Maestri, M., *J. Am. Chem. Soc.* **1979,** *101* (11), 2907-2916; (b) Guldi, D.; Wasgestian, F.; Meyerstein, D., *Inorg. Chim. Acta* **1992,** *194* (1), 15-22; (c) Wieghardt, K.; Schmidt, W.; Herrmann, W.; Kueppers, H. J., *Inorg. Chem.* **1983,** *22* (20), 2953-2956.

18. Baik, M.-H.; Friesner, R. A., *J. Phys. Chem. A* **2002,** *106* (32), 7407-7412.